

ApoE4 reduces glutamate receptor function and synaptic plasticity by selectively impairing ApoE receptor recycling

Ying Chen^{a,1}, Murat S. Durakoglugil^{a,1}, Xunde Xian^{a,1}, and Joachim Herz^{a,b,2}

Departments of ^aMolecular Genetics and ^bNeuroscience, Center for Alzheimer's and Neurodegenerative Disease, University of Texas Southwestern Medical Center, Dallas, TX 75390-9046

Edited by Thomas C. Südhof, Stanford University School of Medicine, Palo Alto, CA, and approved May 21, 2010 (received for review December 25, 2009)

Apolipoprotein E (ApoE) genotype is a powerful genetic modifier of Alzheimer's disease (AD). The ApoE4 isoform significantly reduces the mean age-of-onset of dementia through unknown mechanisms. Here, we show that ApoE4 selectively impairs synaptic plasticity and NMDA receptor phosphorylation by Reelin, a regulator of brain development and modulator of synaptic strength. ApoE4 reduces neuronal surface expression of Apoer2, a dual function receptor for ApoE and for Reelin, as well as NMDA and AMPA receptors by sequestration in intracellular compartments, thereby critically reducing the ability of Reelin to enhance synaptic glutamate receptor activity. As a result, the ability of Reelin to prevent LTP suppression by extracts from AD-afflicted human brains in hippocampal slices from knockin mice expressing the human ApoE4 isoform is severely impaired. These findings show an isoform-specific role of ApoE in the localization and intracellular trafficking of lipoprotein and glutamate receptors and thereby reveal an alternative mechanism by which ApoE4 may accelerate onset of dementia and neuronal degeneration by differentially impairing the maintenance of synaptic stability.

Alzheimer's disease | lipoprotein receptor | neurodegeneration | NMDA receptor | Reelin

ApoE is a lipid transport protein that participates in the regulation of plasma cholesterol, the transport of dietary lipids (1), and protection from atherosclerosis through ApoE receptor-mediated modulation of proliferative signals in smooth muscle cells (2). ApoE is encoded by a single gene and exists in three isoforms (E2, E3, and E4) in the human population, which differ from each other by one or two amino acid substitutions at residues 112 and 158, respectively. The majority of the human population is homozygous for ApoE3 (1). ApoE4 is present in $\approx 16\%$ of the general population and is associated with a significantly earlier average age of onset of dementia, whereas the rare ApoE2 form is protective (3). Differential effects of ApoE isoforms on amyloid- β clearance and the stability of the cytoskeleton have been reported (4), but none of these mechanisms alone can fully explain the molecular basis by which ApoE4 significantly increases Alzheimer's disease (AD) risk.

ApoE receptors are abundantly expressed on neurons in the CNS. As endocytic receptors, they facilitate the transport of synaptogenic cholesterol (5) from astrocytes to neurons, but they also serve as classic signaling receptors for Reelin (6, 7), a ligand that regulates neuronal migration during embryonic development, as well as neurotransmission in the adult brain (8). Reelin activates Src family non-receptor tyrosine kinases (SFKs) through clustering of postsynaptic ApoE receptor-2 (Apoer2) and very-low-density lipoprotein receptor (Vldlr) (8, 9). SFKs subsequently phosphorylate NMDA receptor GluN2 subunits in a highly regulated manner that requires an alternatively spliced sequence motif in the cytoplasmic domain of Apoer2 (10). Reelin thereby potently enhances NMDA receptor activity and increases long-term potentiation (LTP) (reviewed in ref. 8). By contrast, amyloid- β peptide (A β) induces NMDA receptor-dependent synaptic suppression (11) by decreasing GluN2 tyrosine phosphorylation and increasing

endocytosis of the NMDA receptor (12). Reelin and ApoE receptors thus function together to reverse this NMDA receptor-dependent synaptic suppression by doing the opposite—i.e., increasing GluN2 tyrosine phosphorylation (8, 10) and thereby maintaining active NMDA receptors at the neuronal surface (13).

The single amino acid by which ApoE4 differs from ApoE3 radically alters its intracellular trafficking properties. Whereas ApoE3 readily retroendocytoses, ApoE4 remains trapped in endosomes for extended periods of time (14), raising the possibility that neuronal ApoE receptors could also remain sequestered along with ApoE in intracellular compartments in which they are unable to signal to glutamate receptors. Here, we show that ApoE4 preferentially depletes Apoer2, as well as NMDA and AMPA receptors, from the neuronal surface after ligand-induced endocytosis by Reelin. This reduction in signaling competent Apoer2 and surface glutamate receptors is accompanied by a sustained, reduced ability of Reelin to stimulate NMDA receptor-mediated Ca²⁺ influx into cultured neurons. Hippocampal slices from knockin mice expressing the human ApoE4 isoform respond poorly to Reelin and fail to enhance LTP. Moreover, Reelin can effectively reverse the LTP suppression induced by oligomeric A β -containing brain extracts from patients afflicted with AD (13); this is severely impaired in ApoE4 knockin mice. These data show that ApoE4 selectively impairs glutamatergic neurotransmission by reducing ApoE, NMDA, and AMPA receptor functions, thereby facilitating the synaptic suppression mediated by β -amyloid.

Results

We first tested whether the recycling properties of the different ApoE isoforms in primary embryonic cortical neurons from wild-type mice match those reported previously (14). Neurons were incubated for 15 min at 37 °C with identical (3 μ g/mL) concentrations of naturally secreted ApoE2, -E3, or -E4 lipoproteins resembling the small high-density lipoprotein (HDL)-like particles that are generated by astrocytes in the intact brain (15). Surface-bound ApoE was then removed by suramin wash, and cells were chased for an additional 30–120 min. ApoE was then immunoprecipitated from the chase supernatant and cell lysates, and analyzed by immunoblotting (Fig. 1A). Primary mouse cortical neurons do not produce any detectable amounts of ApoE (lanes 1, 5, and 9). Consistent with the earlier reports, ApoE4 release into the culture medium (lanes 4, 8, and 12) during the

Author contributions: Y.C., M.D., X.X., and J.H. designed research; Y.C., M.D., and X.X. performed research; M.D., X.X., and J.H. contributed new reagents/analytic tools; Y.C., M.D., X.X., and J.H. analyzed data; and J.H. wrote the paper.

The authors declare no conflict of interest.

This article is a PNAS Direct Submission.

Freely available online through the PNAS open access option.

¹Y.C., M.S.D., and X.X. contributed equally to this work.

²To whom correspondence should be addressed. E-mail: joachim.herz@utsouthwestern.edu.

This article contains supporting information online at www.pnas.org/lookup/suppl/doi:10.1073/pnas.0914984107/-DCSupplemental.

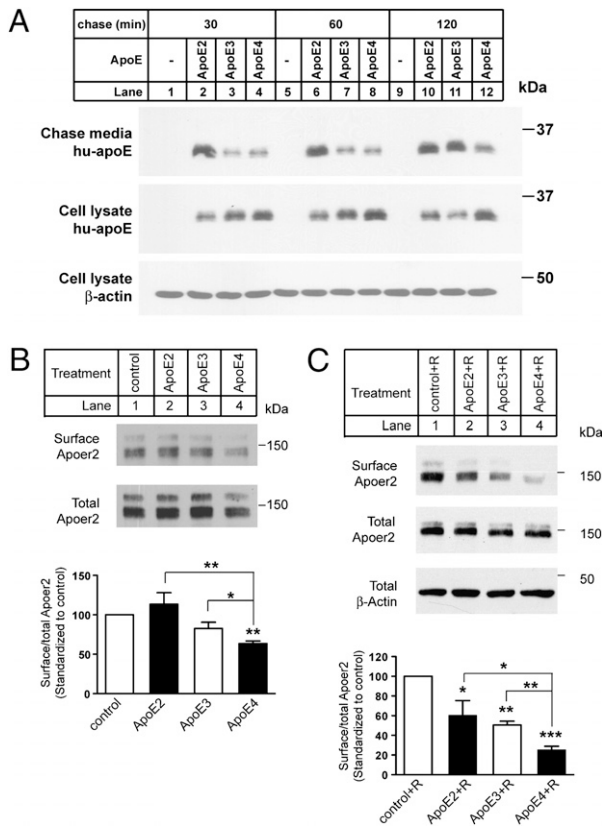


Fig. 1. ApoE4 suppresses neuronal surface expression of Apoer2. (A) Primary neurons were incubated with ApoE at 3 μ g/mL for 30 min at 37 $^{\circ}$ C. Surface-bound ApoE was released by washing the cells with suramin, and neurons were incubated with fresh Neurobasal medium for an additional 30 min, 1 h, or 2 h at 37 $^{\circ}$ C. Media and neuronal lysates were analyzed by immunoblotting for human ApoE or β -actin (loading control). (B) Apoer2 expressed at the plasma membrane of neurons treated with the indicated ApoE isoforms for 15 min at 3 μ g/mL was labeled with membrane-impermeable biotin. Cell lysates were incubated with neutravidin beads, and bound proteins were analyzed by immunoblotting with anti-Apoer2 antibody to visualize surface Apoer2. Total cellular Apoer2 levels were determined by loading 10% of the total cell lysates (Lower). Relative surface Apoer2 levels were determined by normalizing biotinylated Apoer2 levels to the corresponding total Apoer2 levels. Averaged surface Apoer2 levels, which were standardized to control, from four independent experiments are shown. * P < 0.05; ** P < 0.01, compared with control, unpaired t test. (C) Neurons were incubated with 3 μ g/mL ApoE together with Reelin (2 μ g/mL, to stimulate ligand-induced receptor endocytosis) for 2 h at 37 $^{\circ}$ C. Cell lysates were incubated with neutravidin beads, and bound proteins were analyzed by immunoblotting with anti-Apoer2 antibody (Top) to visualize surface Apoer2. Total cell lysates were analyzed directly by immunoblotting for Apoer2 (Middle) or β -actin (loading control, Bottom). Average relative surface levels of Apoer2 were quantitated as described in B. Asterisks above individual columns indicate significant difference compared with control. Asterisks on brackets indicates significant difference between treatments. * P < 0.05; ** P < 0.01; *** P < 0.001.

chase period was markedly delayed compared with ApoE2 (lanes 2, 6, and 10) and ApoE3 (lanes 3, 7, and 11). Substantially more ApoE4 was retained in intracellular compartments at all time points, confirming that impaired recycling of ApoE4 also occurs in primary neurons.

We next used cell-surface biotinylation to test whether this increased sequestration of ApoE4 in intracellular compartments might result in an altered expression of Apoer2 at the plasma membrane (Fig. 1B). Whereas ApoE2 (lane 2) and ApoE3 (lane 3) did not reduce surface expression of Apoer2 compared with the control (lane 1), ApoE4 significantly decreased surface expression

of this “dual function” Reelin and ApoE receptor (lane 4), suggesting that Apoer2 availability, and thus function, at the cell surface might be impaired.

Because Reelin induces endocytosis of its receptors, we tested whether activation of Reelin signaling in the presence of ApoE would further decrease cell-surface expression of Apoer2. All ApoE isoforms (Fig. 1C, lanes 2–4) significantly decreased sur-

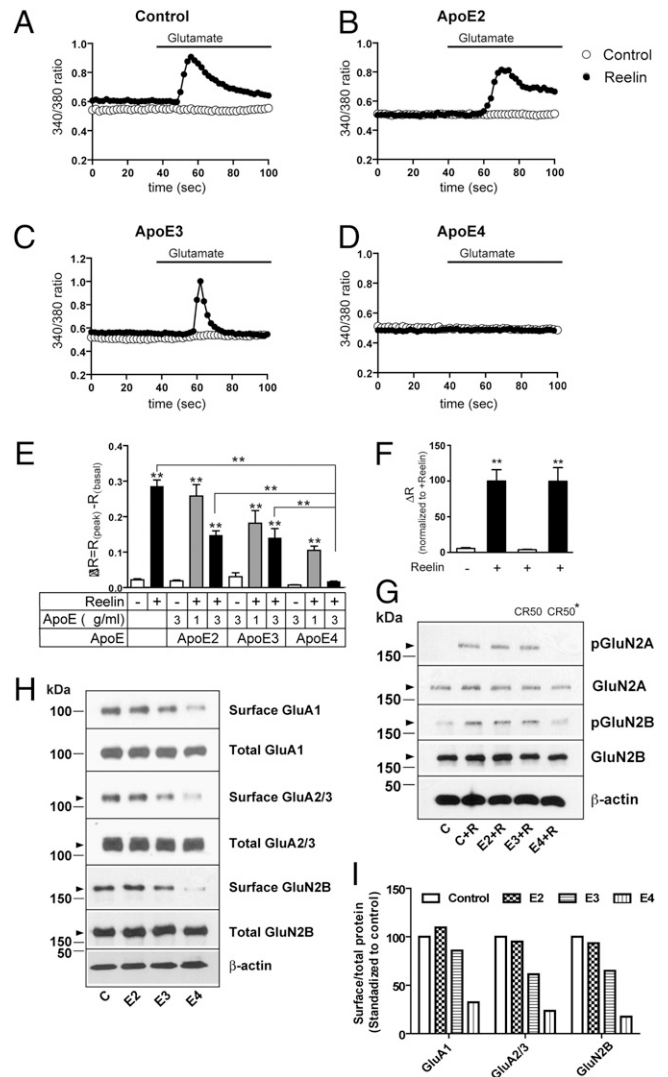


Fig. 2. ApoE4 disrupts Reelin-induced enhancement of NMDA receptor-mediated Ca^{2+} influx, phosphorylation, and glutamate receptor trafficking. Representative traces of fura-2 340/380 ratios recorded from neurons preincubated with media containing (filled circles) or not containing (open circles) 5 nM Reelin and no ApoE (A), or 3 μ g/mL ApoE2 (B), ApoE3 (C), or ApoE4 (D). Response delay due to wash-in of glutamate is \approx 20 s. (E) Averaged ΔR (the maximal difference in 340/380 ratio induced by glutamate) recorded from primary neurons subjected to the indicated treatments in the absence or presence of \sim 5 nM Reelin and 0, 1, or 3 μ g/mL ApoE2, -E3, or -E4 (n = 20–50). Asterisks above individual columns indicate significance (P < 0.001) compared with control neurons receiving no treatment (ApoE nor Reelin). Asterisks on brackets indicate significant difference (P < 0.001) between treatments; unpaired t test. (F) Native but not boiled (CR50*) function blocking CR50 antibody prevents Reelin-dependent Ca^{2+} influx. (G) ApoE4 diminishes Reelin-induced GluN2A and B tyrosine phosphorylation (pGluN2 compared with total cellular GluN2). β -actin, loading control. (H and I) ApoE4 reduces GluA1, GluA2/3, and GluN2B cell-surface levels in acutely Reelin stimulated primary neurons. GluN2A surface levels were too low for reliable detection.

face expression of Apoer2 upon Reelin stimulation compared with control (lane 1). ApoE3 was marginally, but not significantly, more effective than ApoE2, whereas ApoE4 led to a dramatic and statistically highly significant reduction of Apoer2 at the neuronal cell surface. These findings suggested that the activation of NMDA receptors by Reelin, which depends on Apoer2 (10), might be impaired in the presence of ApoE, particularly ApoE4.

We therefore tested whether preincubation with the same ApoE isoforms would also selectively impair Reelin-dependent Ca^{2+} influx into primary cortical neurons evoked by stimulation of NMDA receptors with glutamate (16). In the absence of ApoE preincubation, Reelin robustly increased intracellular, NMDA receptor-dependent Ca^{2+} levels (Fig. 2A). ApoE induced a quantitative reduction in NMDA receptor-dependent Ca^{2+} influx that was isoform-dependent (Fig. 2B–D) and dose-dependent (Fig. 2E). ApoE2 had almost no effect at 1 $\mu\text{g}/\text{mL}$, but at 3 $\mu\text{g}/\text{mL}$ it reduced the maximal response (ΔR) to $\approx 50\%$ of the (no ApoE) control. ApoE3 partially reduced NMDA receptor activity at 1 and 3 $\mu\text{g}/\text{mL}$, whereas ApoE4 substantially decreased intracellular Ca^{2+} levels already at 1 $\mu\text{g}/\text{mL}$ and almost completely abolished NMDA receptor-dependent Ca^{2+} influx at 3 $\mu\text{g}/\text{mL}$. Glutamate-induced Ca^{2+} influx was abolished by the Reelin function blocking CR50 antibody (Fig. 2F). The powerful effect of ApoE4 on NMDA receptor function correlated with the almost complete suppression of Reelin-dependent GluN2 subunit tyrosine phosphorylation (Fig. 2G) and a reduction of not only NMDA but also AMPA receptor subunits at the cell surface (Fig. 2H and I), consistent with the absence of an isoform effect on AMPA/NMDA ratios (Fig. S1 and Tables S1–S4).

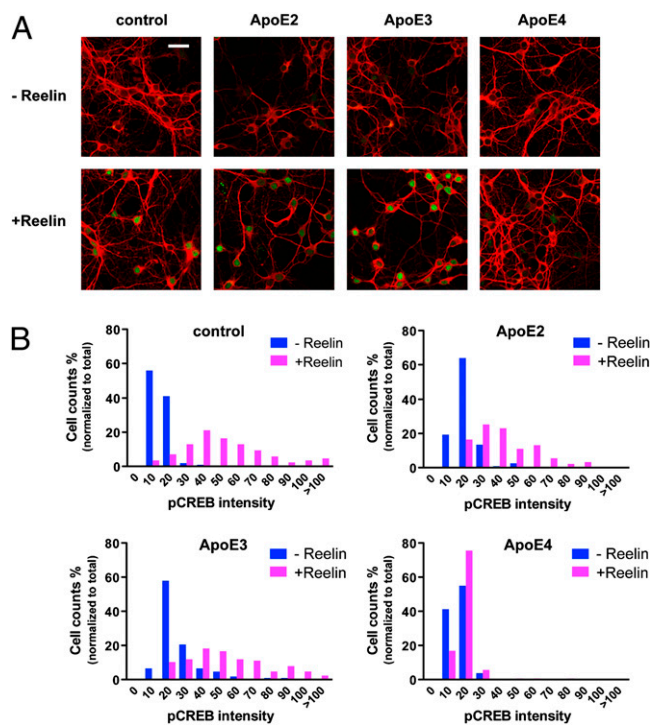


Fig. 3. ApoE4 inhibits Reelin-induced CREB Ser-133 phosphorylation. (A) Confocal microscopy of primary neurons preincubated with ApoE-conditioned media for 10 min, followed by an additional 30-min incubation in the presence or absence of Reelin (2 $\mu\text{g}/\text{mL}$) at 37 $^{\circ}\text{C}$. Neuronal cells were identified using an anti-MAP2 monoclonal antibody (red). Ser-133-phosphorylated nuclear CREB was detected using a polyclonal phosphorylation-site-specific antibody (green). (B) Distribution histogram of nuclear phospho-CREB immunofluorescence in neurons treated as in A. (Scale bar: 30 μm .)

Synaptic NMDA receptor activation is neuroprotective (17) by triggering the phosphorylation of the transcription factor CREB. Reelin greatly increases CREB phosphorylation in response to glutamate (16). Because synaptic dysfunction precedes neuronal death in AD, we decided to investigate whether ApoE4 would also selectively impair nuclear phospho-CREB (pCREB) levels. Cultured cortical neurons were treated as described in Fig. 2, fixed, and stained with a pSer133-CREB-specific antibody. No nuclear pCREB staining was detected in the absence of Reelin (Fig. 3A). By contrast, robust nuclear staining was detected in the presence of Reelin in neurons treated with no ApoE, ApoE2, or ApoE3, but not in neurons exposed to ApoE4. The intensity of nuclear fluorescence was plotted against the number of neuronal nuclei (Fig. 3B). Treatment with ApoE4 essentially abolished nuclear pCREB accumulation.

To determine whether ApoE4 impairs the activity enhancing effect of Reelin on glutamate receptor-dependent synaptic functions (8, 10) to a similar extent *in vivo*, we measured the ability of Reelin to increase θ -burst-induced LTP in the CA1 region in hippocampal slices from homozygous ApoE2, ApoE3, and ApoE4

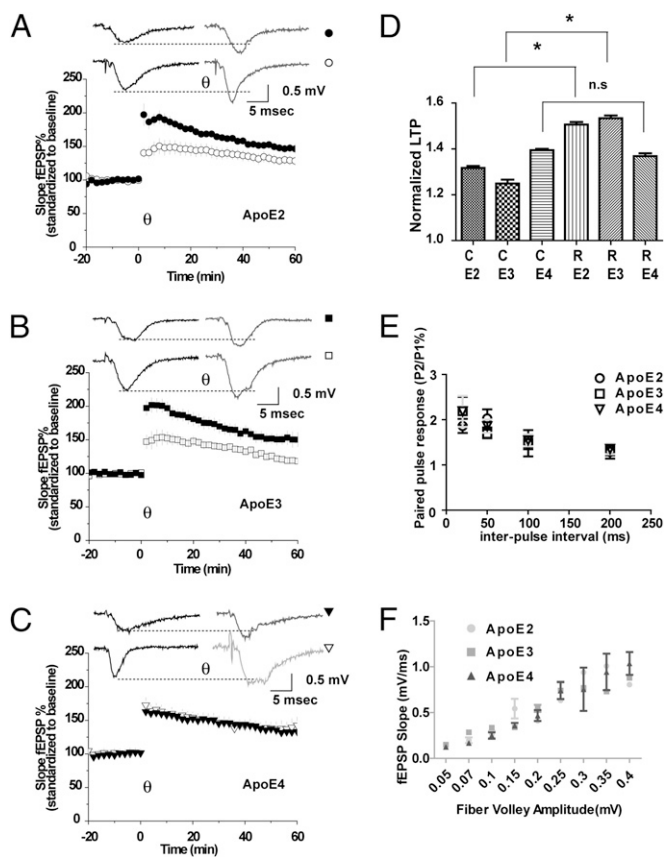


Fig. 4. ApoE4 inhibits Reelin-induced enhancement of long-term potentiation. (A–C) LTP was induced by five trains of θ -burst stimulation of hippocampal slices from knockin mice expressing human ApoE2 (circles, A), ApoE3 (squares, B), or ApoE4 (triangles, C), perfused with control (open symbols: ApoE2, $131.74 \pm 7.52\%$, $n = 12$; ApoE3, $124.9 \pm 3.88\%$, $n = 10$; ApoE4, $139.45 \pm 10.58\%$, $n = 13$) or Reelin-containing (filled symbols, ApoE2, $150.64 \pm 5.7\%$, $n = 6$; ApoE3, $153.36 \pm 9.23\%$, $n = 14$; ApoE4, $136.86 \pm 5.72\%$, $n = 15$) artificial cerebrospinal fluid. Insets show representative traces 10 min before and 30 min after θ -burst in the absence or presence of Reelin. (D) Statistical analysis of slopes 40–60 min after θ -burst stimulation; $*P < 0.05$, ANOVA with Bonferroni's posttests. Asterisk denotes significance ($P < 0.05$). (E) Paired pulse facilitation. Second stimuli delivered at 20, 50, 100, and 200 ms after first stimuli. (F) Input–output curve generated from the fEPSP slope versus fiber volley amplitude measured at increasing stimulus intensities.

ApoE4, but not ApoE2 or ApoE3, significantly impair the ability of synaptic ApoE receptor signaling to counterbalance the synapse depressing effect of A β oligomers.

Discussion

ApoE4 significantly reduces the surface expression of Apoer2 in primary cultured neurons by sequestering the receptor in intracellular recycling compartments. This explains how ApoE isoforms differentially antagonize the activation of NMDA receptor-dependent Ca²⁺ influx by ApoE receptors in a dose-dependent manner. Consequently, in ApoE4 knockin mice, the ability of Reelin to enhance LTP and thereby increase synaptic plasticity in vivo and prevent A β -induced LTP suppression is almost completely abolished.

The cellular mechanisms by which ApoE isoforms differentially affect the age-of-onset of the most common late-onset form of AD have remained unclear. A β peptides bind to ApoE and different ApoE isoforms have been reported to differentially affect the rate of clearance of A β by cells and across the blood-brain barrier (19). ApoE also affects A β fibrillogenesis and plaque formation (20). A β oligomers potently suppress synaptic functions and impair synaptic plasticity (reviewed in ref. 21), and we have recently shown that Reelin signaling through Apoer2 can prevent the A β oligomer-induced inhibition of NMDA receptors at the synapse (13).

In the CNS, ApoE is produced by the glia (reviewed in ref. 4), while multifunctional ApoE receptors are abundantly expressed on the neuronal cell surface where they perform "double duty," mediating lipoprotein uptake as well as signal transduction (8, 16). One of these ApoE receptors, Apoer2, and its ligand Reelin are powerful modulators of NMDA receptor functions in vitro and in vivo (8, 10, 16). Taken together, these findings suggest a possible mechanism by which ApoE isoforms could differentially accelerate synapse dysfunction and AD dementia by interfering with ApoE receptor-dependent neuromodulation (8). Two potential mechanisms by which ApoE might interfere with Reelin signaling are (i) through direct inhibition of binding or (ii) by altering subcellular receptor trafficking. Ligand binding interference is an attractive mechanism that could explain the relative protective effect of ApoE2 over ApoE3. Receptor binding affinity of ApoE2 is reduced

by ≈ 2 orders of magnitude (1). It can, however, not easily explain the powerful disease promoting effect of ApoE4 over ApoE3, because these isoforms bind to receptors with equal affinity (1).

In earlier studies, Heeren et al. (14) have investigated the trafficking properties of ApoE3 and ApoE4 and found a significant accumulation of ApoE4 in intracellular compartments following endocytosis. Taken together, these observations raised the possibility that ApoE4 might also retard ApoE receptor recycling, thereby effectively sequestering a fraction of the receptors inside the cell where they would be unable to signal.

Our findings support such a model (Fig. 6). Exogenously added, naturally secreted ApoE4, but not ApoE2 and ApoE3 lipoproteins significantly decreased neuronal cell surface expression of Apoer2 (Fig. 1) and NMDA receptor mediated Ca²⁺ entry (Fig. 2). Less effective competition by ApoE2 might also manifest itself in this way through reduced interference and higher Ca²⁺ flux. This relative effect of the ApoE isoforms on Reelin and glutamate evoked Ca²⁺ influx intriguingly parallels the order of their relative contribution to AD age-of-onset (3). Moreover, these in vitro findings also bear direct relevance to the function of the intact CNS, where endogenously produced ApoE4, but not ApoE3 or ApoE2 severely impaired the ability of Reelin to enhance hippocampal LTP (Fig. 4) and prevent the synaptic suppression induced by AD brain extract in ApoE4 slices (Fig. 5C).

ApoE levels in total brain extracts average ≈ 5 μ g/mL (22). The ApoE concentrations we have used in this study lie well within this physiological range. Reelin signaling through ApoE receptors thus appears to be one of several physiological components of a kinase network that controls and integrates glutamate receptor-dependent neuronal activity, which is differentially modulated by the effect of ApoE isoforms on ApoE and glutamate receptor trafficking.

From these findings and those of several other groups emerges a picture in which the trafficking of the amyloid precursor protein (APP) and ApoE receptors, ApoE receptor and APP expression, APP processing and A β generation, and modulation of synaptic transmission by ApoE receptors and A β (reviewed in refs. 8 and 21) are cornerstones of an integrated signaling network that is critical for optimizing synaptic responsiveness. Dis-

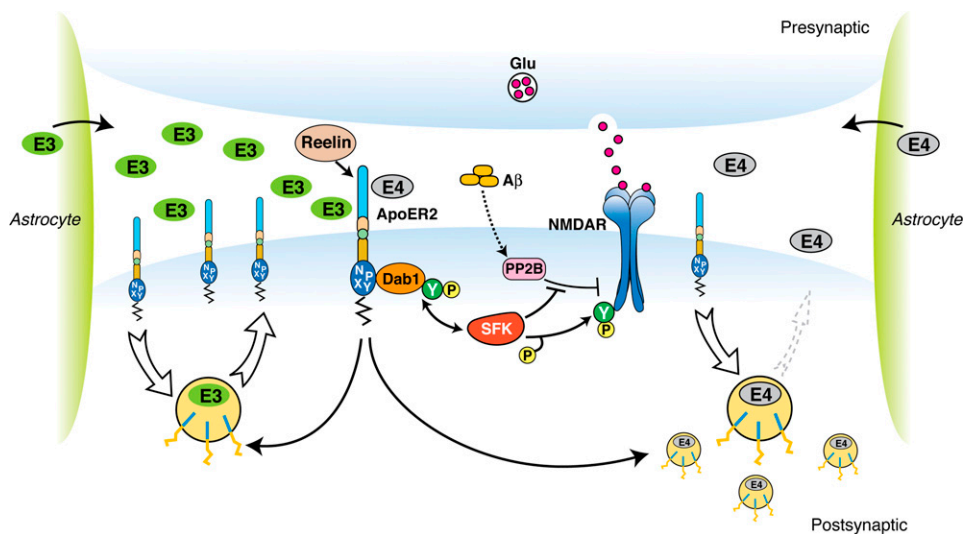


Fig. 6. Effect of ApoE isoforms on ApoE receptor signaling at the synapse. Apoer2 induces NMDAR tyrosine phosphorylation by activating SFKs in response to Reelin in the postsynaptic neuron (8, 10, 16). Astrocyte-derived ApoE3 (green ovals) or ApoE4 (gray ovals) bind to Apoer2 and are constitutively but slowly internalized. Apoer2 undergoes accelerated endocytosis in response to Reelin signaling (Fig. 1) (25). ApoE4 sequesters Apoer2 in intracellular compartments thereby reducing the ability of the postsynaptic neuron to phosphorylate (activate) NMDA receptors in response to Reelin (shown on the right), whereas ApoE2 or ApoE3 efficiently recycle back to the cell surface and thus deplete surface Apoer2 levels to a lesser extent (illustrated on the left for ApoE3). A β oligomers interfere with NMDAR tyrosine phosphorylation by activating tyrosine phosphatases (13, 24).

ruption of this highly interconnected and ordered process may result in a self-reinforcing, progressive synaptic network dysfunction (23) that might accelerate synapse destabilization and neuronal loss. We propose a mechanism (Fig. 6) in which an ApoE isoform-selective impairment of ApoE receptor signaling, through reduced counter regulation of A β induced synaptic depression, ensues a concomitant decrease in synaptic responsiveness. These findings provide a mechanistic rationale that may explain, at least in part, the differential effects of ApoE isoforms on memory, learning, and neuronal survival.

Experimental Procedures

Please refer to *SI Experimental Procedures* for a more extensive description of the experimental procedures used.

ApoE Recombinant Protein Preparation. HEK 293 cells (CRL-1573; ATCC) were transfected using FuGENE 6 reagent with pcDNA3.1 zeo(+), pcDNA3.1 zeo(+)-human ApoE2, pcDNA3.1 zeo(+)-human ApoE3, or pcDNA3.1 zeo(+)-human ApoE4. ApoE lipoproteins were naturally secreted from stably transfected clones at concentrations of ≈ 10 μ g/mL protein in serum-free Neurobasal media.

ApoE Recycling. Primary cortical neurons were cultured for 12–13 d as described in ref. 16, and ApoE trafficking and recycling was determined as described in *SI Experimental Procedures*.

Surface Biotinylation. Surface expression of ApoE receptors was monitored by surface biotinylation and immunoprecipitation as described in detail in *SI Experimental Procedures*.

Calcium Imaging. Reelin- and NMDA receptor-dependent Ca^{2+} influx was determined as described in ref. 16 and in *SI Experimental Procedures*.

Immunocytochemistry. Primary neurons were treated and stimulated as described in *Calcium Imaging* (just above and in *SI Experimental Procedures*). Neurons were fixed and processed with a polyclonal antibody directed against Ser-133 phosphorylated CREB as described in ref. 16.

Hippocampal Slice Preparation and Field Recording. LTP was determined in 2- to 3-month-old mice of the indicated genotype as described in ref. 13 and in *SI Experimental Procedures*.

Preparation of Human Brain Extracts and Prevention of LTP Suppression by Reelin. Human brain extracts from control and histopathologically confirmed AD brain were prepared and their effect on hippocampal LTP was determined as described in ref. 13 and in *SI Experimental Procedures*.

ACKNOWLEDGMENTS. We thank Hui-Chuan Reyna, Wen-Ling Niu, Isaac Rocha, and Priscilla Rodriguez for technical assistance; Mike Brown, Joe Goldstein, Ilya Bezprozvanny, Ege Kavalali, Kim Huber, and Tiina Kotti for critical and constructive comments; and Tom Curran (St. Jude's Hospital, Memphis, TN) and Eckart Förster (University of Hamburg, Hamburg, Germany) for the Reelin expression plasmid and Reelin-producing 293 cells. We are indebted to Patrick Sullivan and Nobuyo Maeda (University of North Carolina, Chapel Hill, NC) for sharing of ApoE knockin mice, to Charles White, Roger Rosenberg, and the Alzheimer's Disease Center at University of Texas Southwestern (Dallas, TX) for providing brain samples, and to Dr. Katsuhiko Mikoshiba (RIKEN, Saitama, Japan) for the function blocking CR50 antibody. This work was supported by grants from the National Institutes of Health, the American Health Assistance Foundation, the Perot Family Foundation, the Consortium for Frontotemporal Dementia Research (CFR), the SFB780, and the Wolfgang-Paul Program of the Humboldt Foundation.

- Mahley RW, Innerarity TL, Rall SC, Jr, Weisgraber KH (1984) Plasma lipoproteins: Apolipoprotein structure and function. *J Lipid Res* 25:1277–1294.
- Herz J, Hui DY (2004) Lipoprotein receptors in the vascular wall. *Curr Opin Lipidol* 15:175–181.
- Corder EH, et al. (1994) Protective effect of apolipoprotein E type 2 allele for late onset Alzheimer disease. *Nat Genet* 7:180–184.
- Mahley RW, Weisgraber KH, Huang Y (2006) Apolipoprotein E4: A causative factor and therapeutic target in neuropathology, including Alzheimer's disease. *Proc Natl Acad Sci USA* 103:5644–5651.
- Mauch DH, et al. (2001) CNS synaptogenesis promoted by glia-derived cholesterol. *Science* 294:1354–1357.
- Trommsdorff M, et al. (1999) Reeler/Disabled-like disruption of neuronal migration in knockout mice lacking the VLDL receptor and ApoE receptor 2. *Cell* 97:689–701.
- Tissir F, Goffinet AM (2003) Reelin and brain development. *Nat Rev Neurosci* 4:496–505.
- Herz J, Chen Y (2006) Reelin, lipoprotein receptors and synaptic plasticity. *Nat Rev Neurosci* 7:850–859.
- Strasser V, et al. (2004) Receptor clustering is involved in Reelin signaling. *Mol Cell Biol* 24:1378–1386.
- Beffert U, et al. (2005) Modulation of synaptic plasticity and memory by Reelin involves differential splicing of the lipoprotein receptor Apoer2. *Neuron* 47:567–579.
- Kamenetz F, et al. (2003) APP processing and synaptic function. *Neuron* 37:925–937.
- Snyder EM, et al. (2005) Regulation of NMDA receptor trafficking by amyloid- β . *Nat Neurosci* 8:1051–1058.
- Durakoglugil MS, Chen Y, White CL, Kavalali ET, Herz J (2009) Reelin signaling antagonizes β -amyloid at the synapse. *Proc Natl Acad Sci USA* 106:15938–15943.
- Heeren J, et al. (2004) Impaired recycling of apolipoprotein E4 is associated with intracellular cholesterol accumulation. *J Biol Chem* 279:55483–55492.
- Koch S, et al. (2001) Characterization of four lipoprotein classes in human cerebrospinal fluid. *J Lipid Res* 42:1143–1151.
- Chen Y, et al. (2005) Reelin modulates NMDA receptor activity in cortical neurons. *J Neurosci* 25:8209–8216.
- Hardingham GE, Bading H (2003) The Yin and Yang of NMDA receptor signalling. *Trends Neurosci* 26:81–89.
- Sullivan PM, Mace BE, Maeda N, Schmechel DE (2004) Marked regional differences of brain human apolipoprotein E expression in targeted replacement mice. *Neuroscience* 124:725–733.
- Zlokovic BV (2008) The blood-brain barrier in health and chronic neurodegenerative disorders. *Neuron* 57:178–201.
- Holtzman DM, et al. (2000) Apolipoprotein E isoform-dependent amyloid deposition and neuritic degeneration in a mouse model of Alzheimer's disease. *Proc Natl Acad Sci USA* 97:2892–2897.
- Haass C, Selkoe DJ (2007) Soluble protein oligomers in neurodegeneration: Lessons from the Alzheimer's amyloid β -peptide. *Nat Rev Mol Cell Biol* 8:101–112.
- Hesse C, et al. (2000) Measurement of apolipoprotein E (apoE) in cerebrospinal fluid. *Neurochem Res* 25:511–517.
- Palop JJ, et al. (2007) Aberrant excitatory neuronal activity and compensatory remodeling of inhibitory hippocampal circuits in mouse models of Alzheimer's disease. *Neuron* 55:697–711.
- Shankar GM, et al. (2008) Amyloid- β protein dimers isolated directly from Alzheimer's brains impair synaptic plasticity and memory. *Nat Med* 14:837–842.
- Morimura T, Hattori M, Ogawa M, Mikoshiba K (2005) Disabled1 regulates the intracellular trafficking of reelin receptors. *J Biol Chem* 280:16901–16908.

Supporting Information

Chen et al. 10.1073/pnas.0914984107

SI Experimental Procedures

ApoE3 and ApoE4 knockin mice are described in refs. 1 and 2. Recombinant Reelin was produced and purified as described in ref. 3. All animal experiments were performed in compliance with the National Institutes of Health Guide for the Care and Use of Laboratory Animals and the procedures approved by the Institutional Animal Care and Use Committees of the University of Texas Southwestern Medical Center.

ApoE Recombinant Protein Preparation. HEK 293 cells (CRL-1573; ATCC) were transfected using FuGENE 6 reagent with pcDNA3.1 zeo(+), pcDNA3.1 zeo(+) human ApoE2, pcDNA3.1 zeo(+) human ApoE3, or pcDNA3.1 zeo(+) human ApoE4. Stably transfected clones were selected in 700 $\mu\text{g}/\text{mL}$ zeocin. HEK 293 cells stably expressing human ApoE or HEK 293 control cells were plated on 10-cm dishes and grown to 80% confluency in low glucose-DMEM containing 10% FCS. Incubation medium was switched to Neurobasal (Invitrogen) and collected 3 d later. Conditioned media as well as ApoE3 standards (Invitrogen) were separated by SDS/PAGE, transferred to nitrocellulose, and blotted with an anti-human ApoE antibody (Calbiochem) and IRDye 800CW secondary antibody (Li-Cor). The band intensity was determined by using the Odyssey infrared imaging system (Li-Cor), and ApoE concentrations were calculated accordingly.

ApoE Recycling. Primary cortical neurons were prepared from embryonic day 18 (E18) embryos and grown in six-well culture dishes as described in ref. 4. At 12–13 d in vitro (DIV), neurons were treated with control (untransfected supernatant) or 3 $\mu\text{g}/\text{mL}$ indicated ApoE isoforms for 15 min at 37 °C. Surface-bound ApoE was removed by suramin, and neurons were incubated with fresh Neurobasal media for an additional 30 min, 1 h, or 2 h at 37 °C. The media were collected and neurons were lysed as described in ref. 4. Media and neuronal lysates were analyzed by Western blot using a polyclonal anti-human ApoE antibody (Calbiochem) and a monoclonal antibody directed against β -actin (Sigma).

Surface Biotinylation. At 12–13 DIV, primary neurons were treated in the absence or presence of 3 $\mu\text{g}/\text{mL}$ indicated ApoE isoforms with or without Reelin for 15 min at 37 °C. Neurons were washed with cold PBS and then incubated in PBS containing 1.5 mg/mL sulfo-NHS-SS-biotin (Pierce) for 30 min at 4 °C. Excess reagent was quenched by rinsing in cold PBS containing 1 mM glycine. Then, 300 μL of lysis buffer [PBS with 0.1% SDS, 1% Triton X-100, and protease inhibitor mixture (Sigma)] was added to the neurons. After 30 min of incubation at 4 °C, lysate was collected and centrifuged at 10,000 $\times g$ for 15 min. Two hundred microliters of cell lysate was incubated with 50 μL of NeutrAvidin agarose (Pierce) at 4 °C for 1 h. Agarose pellets were washed three times in washing buffer [500 mM NaCl, 15 mM Tris-HCl, 0.5% Triton X-100 (pH 8)]. Biotinylated surface proteins were eluted from agarose beads by boiling in SDS sample buffer. Proteins were separated by SDS/PAGE, transferred to nitrocellulose, and blotted with antibodies directed against the ApoE2 carboxyl terminus, GluN2B, GluA1, or GluA2/3, respectively. The data were analyzed by using the Odyssey imaging system (Li-Cor).

NMDA Receptor Phosphorylation Assays. Cortical neurons were incubated with 3 $\mu\text{g}/\text{mL}$ indicated ApoE isoforms and Reelin (5 nM) for 1 h at 37 °C. Four hundred micrograms of protein from cell lysates was incubated with 30 μg of antibodies against GluN2A or GluN2B, respectively, at 4 °C overnight. Immune complexes were precipitated

using 200 μL of protein G-Sepharose slurry (Sigma). Precipitated proteins were analyzed by immunoblotting using a phosphotyrosine-specific antibody (4G10; Upstate Biotechnology) and rabbit polyclonal antibodies directed against GluN2A or GluN2B (Cell Signaling), respectively, as described in ref. 7.

Calcium Imaging. At 12–13 DIV, the primary cortical neurons were preincubated with ApoE for 10 min at 37 °C in artificial cerebrospinal fluid (ACSF) [containing 140 mM NaCl, 5 mM KCl, 2.5 mM CaCl_2 , 1.6 mM MgCl_2 , 10 mM Hepes, and 24 mM D-glucose (pH 7.3)] supplemented with 1 μM tetrodotoxin (Sigma), 5 μM nimodipine (Sigma), and 40 μM 6-cyano-7-nitroquinoxaline-2,3-dione (CNQX) (Sigma). Media containing or not containing 5 nM Reelin and 2 μM fura-2 AM (Molecular Probes) were then applied to the neurons, and recording was started 30 min later. Live-cell images were acquired every 2 s and shown as 340/380 ratios as described in ref. 4. Twenty micromolar glutamate (Sigma) was applied after baseline acquisition. Basal 340/380 ratios [$R(\text{basal})$] were determined as the average of the ratios measured between –15 and –5 s before glutamate application. Peak 340/380 ratios [$R(\text{peak})$] were determined as the maximal ratios 20–60 s after 20 μM glutamate application. ΔR [$\Delta R = R(\text{peak}) - R(\text{basal})$] was defined to indicate the maximal change in 340/380 ratio induced by glutamate. Inhibitors were titrated to isolate Reelin-dependent NMDA receptor response from the Reelin-independent basal NMDA receptor activity.

Immunocytochemistry. Primary neurons were treated and stimulated as described above under *Calcium Imaging*. Neurons were fixed and processed as described in ref. 4. Fixed neurons were incubated with a polyclonal antibody directed against CREB phosphorylated at Ser-133 (1:100 dilution; Cell Signaling Technology) and a monoclonal anti-microtubule-associated protein 2 (MAP2) antibody (1:500 dilution; Sigma) at 4 °C overnight followed by incubation with secondary Cy3-labeled (phospho-CREB) and Cy5-labeled (Map2) antibodies. Fluorescent images were acquired using a Leica TCS SP5 confocal microscopy with a 40 \times objective. Relative fluorescence intensity was quantified using ImageJ software.

Hippocampal Slice Preparation and Field Recording. Two- to 3-month-old mice of the indicated genotype were killed and the brains were rapidly removed. Transverse hippocampal slices (400 μm) were prepared in oxygenated ice-cold dissecting buffer (110 mM sucrose, 60 mM NaCl, 3 mM KCl, 1.25 mM NaH_2PO_4 , 28 mM NaHCO_3 , 0.5 mM CaCl_2 , 7 mM MgCl_2 , 5 mM D-glucose, 0.6 mM ascorbic acid) and processed further as described in ref. 3. Hippocampal slices were allowed to recover in oxygenated ACSF (124 mM NaCl, 5 mM KCl, 1.2 mM NaH_2PO_4 , 26 mM NaHCO_3 , 10 mM D-glucose, 2 mM CaCl_2 , 1 mM MgCl_2) for a minimum of 1 h before recording. Basal synaptic transmission was essentially identical in the ApoE3 and ApoE4 knockin animals, consistent with previously published data (5, 6). Long-term potentiation (LTP) was recorded from CA1 stratum radiatum and evoked by θ -burst stimulation: five trains with an interval of 10 s, each consisting of 10 100-Hz bursts (four pulses) given at 5 Hz. Stimulus intensity was selected to yield 40–60% of the maximal fEPSPs. For Reelin treatment, slices were exposed to Reelin (2 $\mu\text{g}/\text{mL}$ in ACSF) for a minimum of 45 min before θ -burst application. 20/80 slopes of the fEPSPs were used to quantify the magnitude of LTP. The slope of the rising phase of the fEPSP (mV/ms) was measured between 20% and 80% of the peak amplitude and defined as the maximum slope of the response. Potentiation was determined as

the mean fEPSP slope after θ -burst stimulation divided by the mean fEPSP slope determined 20 min before θ -burst stimulation.

Preparation of Human Brain Extracts and Prevention of LTP Suppression by Reelin. Human brain extracts from control and histopathologically confirmed AD brain were prepared and their effect on hippocampal LTP determined as described in ref. 7. Briefly, frozen

human AD and non-AD cortical brain samples (2–4 g) were provided by the University of Texas Southwestern Alzheimer's Disease Center and homogenized in 4 mL/g tissue Tris-buffered saline (TBS) [20 mM Tris-HCl, 150 mM NaCl (pH 7.4)]. Control and Alzheimer patient brain extracts were compared at 5, 25, and 50 μ L/mL perfusate and yielded results that were quantitatively and qualitatively consistent with those reported by Shankar et al. (8).

1. Sullivan PM, et al. (1997) Targeted replacement of the mouse apolipoprotein E gene with the common human APOE3 allele enhances diet-induced hypercholesterolemia and atherosclerosis. *J Biol Chem* 272:17972–17980.
2. Wang C, et al. (2005) Human apoE4-targeted replacement mice display synaptic deficits in the absence of neuropathology. *Neurobiol Dis* 18:390–398.
3. Weeber EJ, et al. (2002) Reelin and ApoE receptors cooperate to enhance hippocampal synaptic plasticity and learning. *J Biol Chem* 277:39944–39952.
4. Chen Y, et al. (2005) Reelin modulates NMDA receptor activity in cortical neurons. *J Neurosci* 25:8209–8216.
5. Kitamura HW, et al. (2004) Age-dependent enhancement of hippocampal long-term potentiation in knock-in mice expressing human apolipoprotein E4 instead of mouse apolipoprotein E. *Neurosci Lett* 369:173–178.
6. Trommer BL, et al. (2004) ApoE isoform affects LTP in human targeted replacement mice. *Neuroreport* 15:2655–2658.
7. Durakoglugil MS, Chen Y, White CL, Kavalali ET, Herz J (2009) Reelin signaling antagonizes β -amyloid at the synapse. *Proc Natl Acad Sci USA* 106:15938–15943.
8. Shankar GM, et al. (2008) Amyloid- β protein dimers isolated directly from Alzheimer's brains impair synaptic plasticity and memory. *Nat Med* 14:837–842.

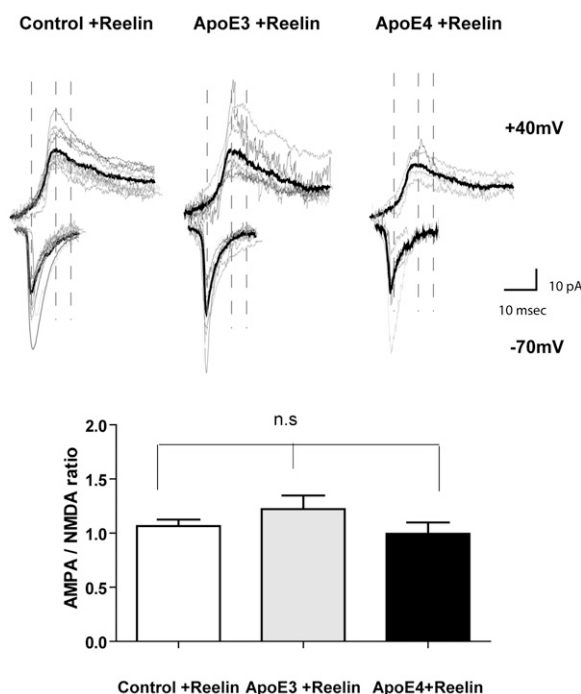


Fig. S1. Whole-cell recordings and determination of AMPA/NMDA ratios. Single cells were recorded from 13- to 21-DIV primary hippocampal neurons. ApoE3, ApoE4, or control medium was applied together with Reelin (5 nM) 30 min before the recordings started. Extracellular solution contained 140 mM NaCl, 5 mM KCl, 2.5 CaCl₂, 1.6 mM MgCl₂, 10 mM Hepes, and 24 mM D-Glucose (pH 7.3); intracellular solution contained 135 mM CsCl, 10 mM Hepes, 1 mM CaCl₂, 2 mM MgCl₂, 2 mM TEA, 0.5 mM EGTA, 4 mM MgATP, 10 mM creatinine phosphate, 5 mM QX314, and 0.3 mM GTP. Spontaneous synaptic activity from the indicated number of individual neurons was determined at 30 °C in the presence of picrotoxin (50 μ M), nimodipine (5 μ M), and TTX (0.5 μ M). Minis were analyzed over a time period of 1 min and averaged using a template in P-clamp 10. AMPA over NMDA ratios were calculated as the peak of the response at -70 mV over the response 10–15 ms after the peak at +40 mV. ANOVA, $P > 0.05$; ApoE3, 1.22 ± 0.12 , $n = 10$; ApoE4, 0.99 ± 0.1 , $n = 9$; Control, 1.06 ± 0.06 , $n = 13$.

Table S1. Evoked EPSCs in primary cultured neurons were recorded and peak amplitudes were plotted at different holding potentials

Holding potentials	ApoE3 + Reelin ($n = 4$)	ApoE4 + Reelin ($n = 4$)
-70 mV	-48.85 \pm 22.26	-22.90 \pm 10.22
+40 mV	118.80 \pm 44.98	105.18 \pm 45.05

Ten micromolar CNQX, 50 μ M picrotoxin, and 5 μ M nimodipine were added to isolate NMDA currents. Evoked currents were induced with high (10–20 mA) stimulation intensities, resulting in recurrent network activity and asynchronous release, which prevented reliable data analysis. We therefore decided to record spontaneous activity in the presence of TTX (Tables S2–S4) to obtain an estimate of the effect of ApoE4 on AMPA and NMDA currents.

Table S2. Peak amplitude (pA) values of mixed mEPSCs recorded in the presence of TTX, picrotoxin, and nimodipine under the indicated conditions (no ApoE, ApoE3, and ApoE4) and holding potentials

Holding potentials	Control + Reelin (n = 13)	ApoE3 + Reelin (n = 10)	ApoE4 + Reelin (n = 8)
-70 mV	-15.53 ± 1.15	-17.39 ± 2.18	-12.70 ± 1.99
+40 mV	14.79 ± 0.979	15.39 ± 2.25	12.54 ± 1.19

Minis were analyzed using a template in pClamp10. ApoE4 reduced currents at both holding potentials.

Table S3. Minis were recorded in the presence of DAP5 to isolate AMPA currents at -70 mV

Holding potentials	ApoE3 + Reelin (n = 4)	ApoE4 + Reelin (n = 2)
-70 mV	-13.95 ± 2.63	-8.87 ± 0.27

Similarly, ApoE4 treatment in the presence of Reelin reduced currents.

Table S4. AMPA over NMDA ratios under the indicated conditions

Treatments mEPSCs	Control + Reelin (n = 13)	ApoE3 + Reelin (n = 10)	ApoE4 + Reelin (n = 8)
AMPA/NMDA ratios	-2.28 ± 0.19	-2.65 ± 0.29	-2.01 ± 0.36

NMDA currents were calculated from the mixed minis 40–45 ms after response onset.